CIRCUIT SIMULATION OF THE MITL IN AN IVA WITH A NON-IDEAL CENTER CONDUCTOR *

Raymond Allen, Paul Ottinger, and Joseph Schumer
Plasma Physics Division
Naval Research Laboratory
Washington, DC 20375 USA

Abstract

The present MITL center conductor of the Mercury IVA tapers down in diameter at each cell feed so as to have the ideal, uniformly increasing steps in impedance as the line voltage increases. This provides optimal power coupling to a self-limited load and ensures that electron flow will not be lost at the impedance transitions of the MITL, thereby retaining magnetic insulation. The output voltage of Mercury into a self-limited load can be increased by decreasing the diameter of the center conductor, increasing the MITL impedance. A simple, low-cost way to do this is to reuse some segments of the existing center conductor, even though they have non-ideal diameters in this new configuration, and add a few, smaller diameter components. However, impedance mismatches and current loss down the MITL can reduce the output voltage in this non-ideal case. So, simulations were required to verify that the new MITL would still be magnetically insulated and efficiently couple power to the load. A new MITL circuit element that has variable impedance and that can model current loss at non-ideal impedance transitions was used in a transmission-line circuit code to quickly evaluate possible combinations of new and existing center conductor elements. In two MITL configurations tested, insulation (or the loss thereof) and power coupling predicted in the circuit code was verified by PIC simulations using LSP.

I. INTRODUCTION

Circuit modeling of an IVA (inductive voltage adder), such as Mercury [1], is complicated by the magnetically-insulated electron flow in the adder and in the MITL (magnetically-insulated transmission line) output line. Electron flow reduces the impedance of transmission lines below their vacuum value, Z_0. An accurate representation of MITL elements in a circuit code requires transmission line elements with variable effective impedance. This effective impedance is given by the flow impedance, Z_F, from Mendel MITL theory given by

$$Z_F \equiv Z_0 \frac{\langle E \rangle}{E_A} = \frac{V}{\sqrt{I_A^2 - I_C^2}} \quad (1)$$

where <E> is the average electric field between inner and outer conductors, E_A is the electric field at the anode surface, I_A is the current on the anode, and I_C is the current on the cathode. The difference between I_A and I_C equals the electron flow current.

In addition to variable impedance, a MITL circuit element requires a variable loss term for accuracy. This loss term represents electron loss to the anode. When insulated, there is no loss. However, there are three times or positions where loss is present. First, when voltage is first applied to the line, there is a transition from space charge limited loss to no loss as the line becomes insulated. Second, current can be shed to the anode at the end of the line. Often, the load at the end of the line has an impedance greater than the self-limited flow impedance and the line operates in a "self limited" mode. In this case, the effective impedance of the line is the self-limited impedance and current, not going into the load, is shed to the anode. So, the MITL circuit element at the end of the line must be able to correctly represent the loss term for load impedances greater to or less than the self-limited impedance. The third area where losses are important is at "bad transitions". Bad transitions occur when the flow moves from a lower impedance line to a higher impedance line. As will be shown later, the MITL circuit model described here will require improvements to correctly handle bad transitions.

One area in which this new model has already contributed is in the design of a modified center conductor for Mercury. Simple modifications to the existing center conductor can increase the output voltage. However, care must be taken not to exceed the voltage ratings of the individual cells. Also, it was believed that one must avoid bad transitions that lead to current loss in the adder.

Because of non-uniform impedance steps in an easily modified center conductor, it is difficult to determine the exact cell voltages and the presence of any current losses without modeling, using either a circuit code or a PIC (particle-in-cell) code. Although the PIC code LSP [2] is known to be accurate and therefore used as a benchmark

* Work supported by the UK Atomic Weapons Establishment and the US DOE through Sandia National Laboratories.

Report Documentation Page

Form Approved
OMB No. 0704-0188

1. REPORT DATE	2. REPORT TYPE	3. DATES COVERED
JUN 2007	**N/A**	**-**

4. TITLE AND SUBTITLE
Circuit Simulation Of The Mitl In An Iva With A Non-Ideal Center Conductor

5a. CONTRACT NUMBER
5b. GRANT NUMBER
5c. PROGRAM ELEMENT NUMBER

6. AUTHOR(S)

5d. PROJECT NUMBER
5e. TASK NUMBER
5f. WORK UNIT NUMBER

7. PERFORMING ORGANIZATION NAME(S) AND ADDRESS(ES)
Plasma Physics Division Naval Research Laboratory Washington, DC 20375 USA

8. PERFORMING ORGANIZATION REPORT NUMBER

9. SPONSORING/MONITORING AGENCY NAME(S) AND ADDRESS(ES)

10. SPONSOR/MONITOR'S ACRONYM(S)
11. SPONSOR/MONITOR'S REPORT NUMBER(S)

12. DISTRIBUTION/AVAILABILITY STATEMENT
Approved for public release, distribution unlimited

13. SUPPLEMENTARY NOTES
See also ADM002371. 2013 IEEE Pulsed Power Conference, Digest of Technical Papers 1976-2013, and Abstracts of the 2013 IEEE International Conference on Plasma Science. IEEE International Pulsed Power Conference (19th). Held in San Francisco, CA on 16-21 June 2013., The original document contains color images.

14. ABSTRACT
The present MITL center conductor of the Mercury IVA tapers down in diameter at each cell feed so as to have the ideal, uniformly increasing steps in impedance as the line voltage increases. This provides optimal power coupling to a self-limited load and ensures that electron flow will not be lost at the impedance transitions of the MITL, thereby retaining magnetic insulation. The output voltage of Mercury into a self-limited load can be increased by decreasing the diameter of the center conductor, increasing the MITL impedance. A simple, low-cost way to do this is to reuse some segments of the existing center conductor, even though they have nonideal diameters in this new configuration, and add a few, smaller diameter components. However, impedance mismatches and current loss down the MITL can reduce the output voltage in this non-ideal case. So, simulations were required to verify that the new MITL would still be magnetically insulated and efficiently couple power to the load. A new MITL circuit element that has variable impedance and that can model current loss at non-ideal impedance transitions was used in a transmission-line circuit code to quickly evaluate possible combinations of new and existing center conductor elements. In two MITL configurations tested, insulation (or the loss thereof) and power coupling predicted in the circuit code was verified by PIC simulations using LSP.

15. SUBJECT TERMS

16. SECURITY CLASSIFICATION OF:			17. LIMITATION OF ABSTRACT	18. NUMBER OF PAGES	19a. NAME OF RESPONSIBLE PERSON
a. REPORT **unclassified**	b. ABSTRACT **unclassified**	c. THIS PAGE **unclassified**	**SAR**	**7**	

Standard Form 298 (Rev. 8-98)
Prescribed by ANSI Std Z39-18

for the circuit model, an accurate circuit model is also desired because it is much faster to setup and run.

A. Ideal Voltage Adder

Normally, the center conductor of an IVA tapers down after each cell from the ground end to the load end. The idea is to form a transmission-line voltage adder [3]. In an ideal six-stage transmission-line voltage adder, shown in Fig. 1a, there are six identical sources feeding the adder through six lines of the same impedance, Z_{Feed}. The feeds are connected by elements, MITL1...MITL6, that represent the MITLs after each cell feed formed by the central bore and center conductor of the IVA. If the MITL impedances are designed to increase in equal steps (and if the voltage sources are staggered properly in time), then the adder can be represented by the simple equivalent circuit of Fig. 1b.

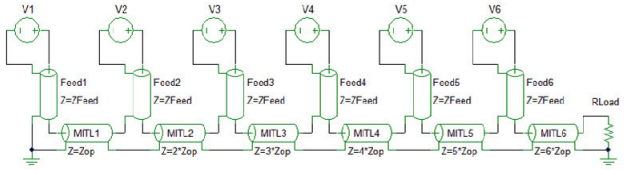

a)

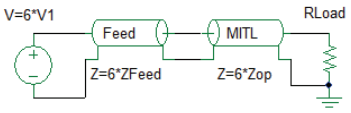

b)

Figure 1. Transmission-line adder representation of an ideal six-stage IVA (a) and the equivalent circuit (b).

The MITL impedance steps are normally designed to be of equal Z_{Op} [4], the operating impedance of the line determined using the Creedon MITL theory [5] defined by

$$Z_{Op} = \left.\frac{V}{I_A}\right|_{Self-Limited} = f(V, Z_0) \qquad (2)$$

where V is the MITL voltage and I_A is the anode current when the line is running self-limited. Z_{Op} is a function only of the voltage and the vacuum impedance of the MITL, Z_0.

Generally, the design procedure is to first assume that the IVA is operating into a self-limited load such that $R_{Load}=6*Z_{Op}$ in Fig. 1a. Then, if V1…V6 are all equal forward-going wave voltages feeding the adder, the steps in adder voltage, V, are given by

$$V_{Step} = V_1 \frac{2Z_{Op}}{Z_{Op} + Z_{Feed}} \quad . \qquad (3)$$

and, from the circuit in Fig. 1b, it is clear that the self-limited load voltage for the six-stage adder is just six times V_{Step} of Eq. (3). So, assuming that Z_{Feed} is fixed, one decides on a value for Z_{Op} that gives the desired load voltage into a self-limited load. Then, the vacuum impedances, Z_0, of each MITL segment can be calculated using the Creedon theory. This gives the diameters of center conductor segments required, assuming that the bore diameter is fixed.

It could be argued that the effective impedance of an MITL is better represented by Mendel's Z_F, so that it may be better to design the adder for equal steps of the self-limited impedance, Z_F^{SL}, rather than in steps of Z_{Op}. However, Z_F^{SL} and Z_{Op} are nearly equal.

B. Non-Ideal Voltage Adder

The transmission-line voltage adder shown in Fig. 1a is non-ideal if either the feed impedances are not identical or the steps in MITL impedances are not equal. In either case, the simplified representation of Fig. 1b is no longer valid. The voltages developed at each of the feeds will not be the same. Also, there is the possibility of the loss of electron flow current at bad MITL junctions (discussed later).

II. MERCURY CENTER CONDUCTOR DESIGN FOR 8-MV OPERATION

One of the first test applications of the new MITL circuit model, described later, was the design of a higher voltage center conductor for Mercury to increase the expected output from the current 7 MV to 8 MV. Raising Z_{Op} by narrowing the center conductor increases the voltage into a self-limited load. But, the Mercury feeds have a design limit of 1.3 MV. So, the maximum safe output voltage is about 8 MV with six cells. A careful look at the existing Mercury center conductor shows that several sections are close in diameter to that required for an ideal 8-MV center conductor. The new MITL circuit model as well as PIC simulations were used to investigate the possibility of simply modifying the existing center conductor for 8 MV operation.

The existing center conductor for Mercury was designed for positive polarity, but is being used in negative polarity. In negative polarity, all flow electrons originate from the center conductor, at the same potential, and the flow stays near the center conductor. However, in positive polarity flow electrons fill the AK gap as they originate from the outer conductor at different potentials after every feed and the flow current is much higher. As a result, the existing Mercury adder is not ideal in negative polarity. However, it has been found that the deviation from ideal has had minimal impact. Several simulations and measured data show that there is no flow loss, the cell voltages are similar, and the simplified representation of Fig. 1b is fairly accurate. A diagram of the vacuum

impedances of the existing center conductor and also that of an ideal one with the same 30-Ω output Z_0 is shown in Fig. 2. Calculations give a Z_{Op} of 24 Ω for this Z_0 and a 7-MV voltage, which yields 4-Ω steps in Z_{Op} for the ideal center conductor (used to calculate Z_0 for sections of the ideal line).

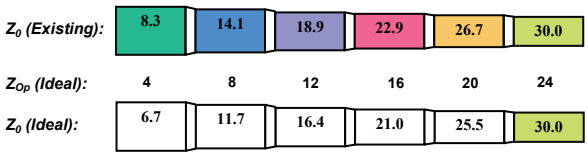

Figure 2. Diagrams of the existing Mercury center conductor sections (above) with corresponding Z_0 and the ideal center conductor (below) for the same 7-MV output voltage and same 30-Ω output Z_0. Also shown are the steps in Z_{Op} for the ideal line.

Increasing the nominal output voltage to 8 MV requires increasing the ideal steps in Z_{Op} from 4 to 5.22 Ω. From a comparison of the resultant vacuum impedances to that of the existing center conductor, shown in Fig. 3, it is evident that several sections are very near to the ideal for 8 MV output, meaning that their physical outer diameters are very near to that desired. This is especially true for those segments near the base (left side in Fig. 3). These segments are the most expensive to design and fabricate as they are the largest diameter and experience the most physical stress. In particular, a great deal of expense and design time would be saved if the left most piece of the existing center conductor could be used as this piece connects to the support hardware, connects to ground, and has holes for vacuum pumping.

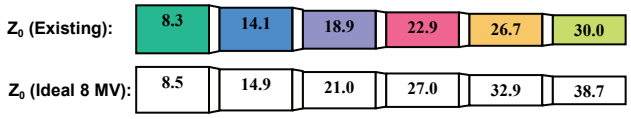

Figure 3. Diagrams of the existing Mercury center conductor sections (above) with corresponding Z_0 and the ideal center conductor (below) for 8-MV output voltage.

There were several possibilities investigated for the conversion to 8 MV, ranging from keeping only the left-most section to simply replacing the last section. A circuit model is very useful because circuit simulations only require seconds or minutes instead of the hours or days required by PIC simulations. Many simulations of both types were performed to investigate all the possibilities and the impact on output voltage, cell voltage, and flow insulation. The results are discussed later, after describing the MITL circuit model element used in the analysis and its limitations.

III. MITL CIRCUIT MODEL

A new MITL circuit model element is being developed to more quickly, easily, and accurately model IVAs. The model is based on equations from Ottinger [6], derived from Mendel theory. Each MITL element in the circuit model is subdivided into single time-step elements with a downstream resistance. The impedance of every element is variable, given by Z_F (Eq. (1)). The downstream resistance, R_{Loss}, is used to represent any electron loss to the anode.

A. MITL Circuit Model Details

Each element calculates a new Z_F and R_{Loss} at every time step. It is an explicit solution as it uses the voltage and current (at the downstream end) calculated from the previous time step to calculate new Z_F and R_{Loss} values. Given V and Z_0, the self-limited anode current, I_{ASL}, of the element is calculated using Ref. [6]. If the anode current of the element, I_A, is greater than I_{ASL}, then the element is insulated and the new value for Z_F is determined via Mendel theory. Note that the insulated $Z_F(I_A)$ for a given V and Z_0 is double valued with "super-insulated" and a "saturated" flow branches as shown in Fig. 4.

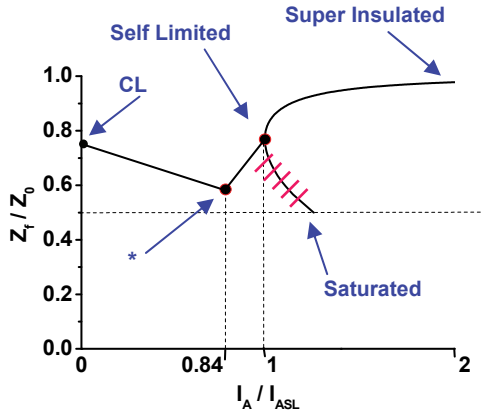

Figure 4. Example plot of Z_F versus I_A (scaled by I_{ASL}) used by the circuit model for a given V and Z_0.

Because earlier PIC simulations indicated that the flow (for Mercury in negative polarity) was mostly in the super-insulated state, it was decided, for simplicity, to ignore the saturated solution and make $Z_F(I_A)$ single valued. Unfortunately, it has been found that the flow does move to the saturated branch when bad transitions are present. So, as discussed later, a more sophisticated model will be required to properly handle bad transitions.

A recent study of LSP simulations shows that the self-limited point is not exactly at the minimum current, as shown in Fig. 4, but somewhat on the saturated branch [7]. Consequently, the model has a slight error, described later, when compared with LSP.

The model must also assign Z_F values to the element when $I_A<I_{ASL}$. It was decided to use Eq. (1) in this regime also. However, there are only two points where Z_F is easily calculated. For $I_A=0$ a value for Z_F was calculated via the well known Child-Langmuir self-limited current theory (even though the actual geometry is cylindrical rather than planar). Since,

$$\Phi(x) = V\left(\frac{x}{D}\right)^{4/3}$$

$$E_x(x) = \frac{-d\Phi(x)}{dx} = -\frac{4}{3}\frac{V}{D}\left(\frac{x}{D}\right)^{1/3}$$

$$E_x(D) = -\frac{4}{3}\frac{V}{D} = \frac{4}{3}\langle E\rangle$$

where Φ is the potential, E_X is the electric field, x=0 is the cathode and x=D is the anode, then Z_F is just ¾ of Z_0 from

$$Z_F{}^{CL} \equiv Z_0\left(\frac{\langle E\rangle}{E_x(D)}\right) = \frac{3}{4}\cdot Z_0 \ . \qquad (3)$$

In a similar way, Z_F is calculated at a second point, (indicated by "*" in Fig. 4) corresponding to the point $\omega_{ce}{}^{(1)}$ from Ref. [8], where $\omega_{ce}{}^{(1)}=0.84\cdot\ \omega_{ce}{}^{crit}$ and $\omega_{ce}{}^{crit}$ is the critical point. For the purposes of this model, the critical point is equated to the self-limited point, although this is known to be an approximation. Since ω_{ce} is proportional to the magnetic field generated by I_A, we have $I_A{}^* = 0.84\cdot I_{ASL}$. It is found that

$$E_x(D) = \frac{-d\Phi(D)}{dx} = -\frac{m_e D}{e}\left(\omega_{ce}^1\right)^2$$

$$= -0.84\frac{m_e D}{e}\left(\frac{2eV}{D^2 m_e}\right) = 1.66\langle E\rangle.$$

So,

$$Z_F{}^* \equiv Z_0\left(\frac{\langle E\rangle}{E_x(D)}\right) = 0.60\cdot Z_0 \qquad (4)$$

at the point $\omega_{ce}{}^{(1)}$. For other values of $I_A<I_{ASL}$, Z_F is determined by linear interpolation between $Z_F{}^{CL}$, $Z_F{}^*$, and $Z_F(I_{ASL})$ as shown in Fig. 4.

Calculating a new value for the loss resistance, R_{Loss}, is more complicated because it depends on the condition of downstream element. So first, every element calculates a maximum loss current, $I_{LossMax}$. The actual loss current for each element, I_{Loss}, is then calculated as $I_{LossMax}$ minus any current taken up by the downstream element and $R_{Loss}=V/I_{Loss}$.

An example plot of $I_{LossMax}$ for a fixed V and anode and cathode dimensions is shown in Fig. 5. For $I_A>I_{ASL}$, the maximum loss current is simply I_{ASL}. For $I_A<I_{ASL}$, the value is interpolated between the same I_A values as with Z_F. For $I_A=0$, $I_{LossMax}$ is I_{LB}, the Langmuir-Blodgett space-charge-limited current [9]. For $I_A=I_A{}^*$, the loss current is given by Ref. [8] to be 0.86 times I_{LB}.

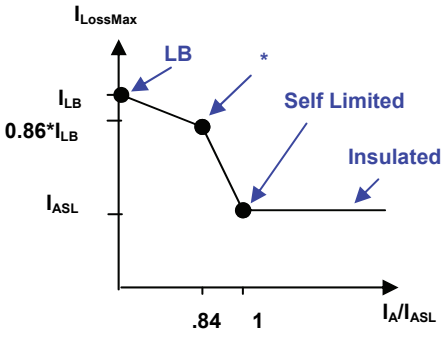

Figure 5. Example plot of $I_{LossMax}$ versus I_A (scaled by I_{ASL}) used by the circuit model for a given V and dimensions of anode and cathode.

For the last element (most downstream), with no attached load, $I_{Loss}=I_{LossMax}$, because all anode current must consist of electron flow from the cathode. With a load attached to the last element, I_{Loss} is reduced by up to the load current, $I_{Load}=V/R_{Load}$, depending on I_A. If $I_A>I_{ASL}$, then $I_{Loss}=\max[0,I_{LossMax}-I_{Load}]$ as up to $I_{LossMax}$ is diverted to the load. If $I_A=0$, then $I_{Loss}=I_{LossMax}$ as no current is diverted to the load. For $0<I_A<I_{ASL}$, an approximation, $I_{Loss}=\max[0,I_{LossMax}-I_{Load}*I_A/I_{ASL}]$, is used. So, in general,

$$I_{Loss}=\max[0,I_{LossMax}-I_{Load}*F(I_A/I_{ASL})] \qquad (5)$$

where $F(x)=\min[x,1]$. In some cases, it is desirable to have the load resistance represent a radiographic diode that accepts only bound current and sheds all flow current. For this case I_{Loss} is given by

$$I_{Loss}=\max[I_{LossMax}, \mathrm{sqrt}((I_{Load})^2+(V/Z_F)^2)] - I_{Load} \qquad (6)$$

For upstream elements, the I_{Loss} is reduced not by the load current, but by the maximum loss current allowed by the downstream element. In this case, Eq. 5 is used with I_{Load} replaced by $I_{LossMax}$ of the downstream element.

B. MITL Circuit Model Limitations

This MITL circuit model element has other limitations in addition to those already discussed. First, the state of each element would oscillate at the time step rate. To counter this behavior, the two state variables of each element, Z_F and $I_{LossMax}$, are only allowed to take Newtonian half steps toward their new value at each time step. This produces a much smoother output but limits the temporal fidelity.

Second, the model works best for longer time step values when the most downstream element must shed a lot of flow current, as in the case of self-limited operation. When running self-limited, the state of the most

downstream element is right at the edge of insulation and the result is found to be most stable when this element is long enough so that it can shed the entire self-limited current, even when not insulated. Otherwise, two or more elements compete to shed the flow. For simulating Mercury, a minimum time step of 0.5 ns works best.

Also, this model assumes that power flow is in one direction as the loss resistor of each element is only on the downstream end. So, care must be taken when constructing the model.

IV. MITL CIRCUIT MODEL BENCHMARKS

The MITL circuit model was benchmarked against PIC simulations and analytic solutions. The first tests compared the steady-state solutions from a PIC simulation of a MITL with a variable load to a corresponding circuit simulation and the analytic results from both Creedon and Mendel theories. Later, the temporal behavior of PIC and circuit IVA simulations is compared. The MITL circuit model element was added to the circuit code CASTLE (Circuit Analysis and Simulation with Transmission-Line Emphasis), a modified nodal analysis code with special handling for transmission lines.

The first benchmark was for a simple, constant 30-Ω vacuum impedance MITL fed by a 30-Ω source with a fast ramp to a constant 6-MV injected voltage wave. In the PIC simulations, inner and outer conductors are terminated in plates that form an AK gap that was adjusted to give variable load impedance. Particle plots from the PIC code showing the physical geometry simulated and a schematic from CASTLE showing the equivalent circuit are shown in Fig. 6. The PIC simulation was run with four different AK gaps, one large enough so that the MITL ran in self-limited mode, and three smaller gaps. The load impedance for the smaller gaps, calculated from the PIC output, was used as the load resistance in CASTLE simulations and analytic calculations for comparison.

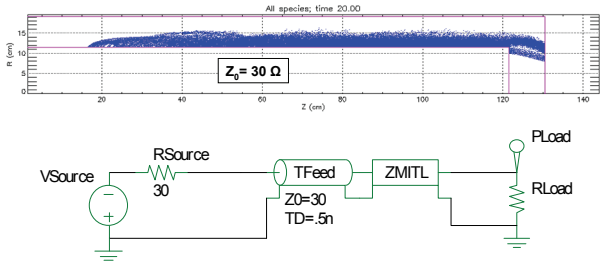

Figure 6. Particle plot showing the setup from PIC simulation of a constant 30-Ω MITL (above) and the equivalent CASTLE circuit schematic (below).

A comparison of anode and flow currents for each of the four load conditions is shown in Fig. 7. All anode current solutions lie, as they should, along the load line given by the 6-MV forward-going wave source with 30-Ω impedance and higher flow current. There is generally quite good agreement between LSP, CASTLE, and analytic solutions. However, for the self-limited case, the LSP solution has slightly lower impedance. It is believed that by using a rescaled Mendel flow theory [7] both the CASTLE and analytic Mendel solutions would agree with LSP.

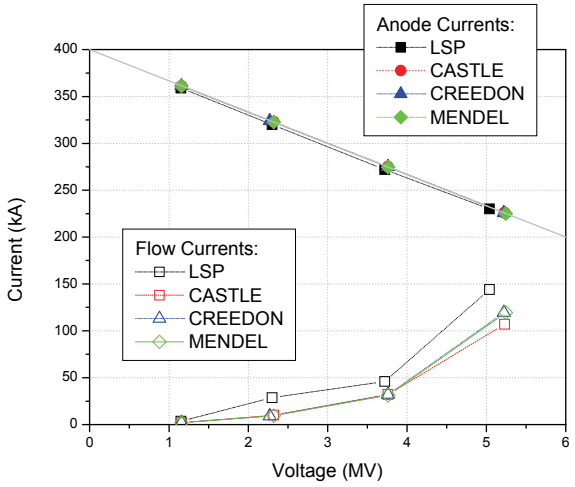

Figure 7. Comparison of anode and flow currents versus voltage for PIC and CASTLE simulations and also analytic calculations using Creedon and Mendel theories.

The second benchmark was the same MITL with a lower impedance, 14.3-Ω MITL connected downstream. This represents a good transition where no flow current is expected to be lost. The results for the self-limited case and one loaded case are shown in Fig. 8. The results agree as they did in the case of the first benchmark.

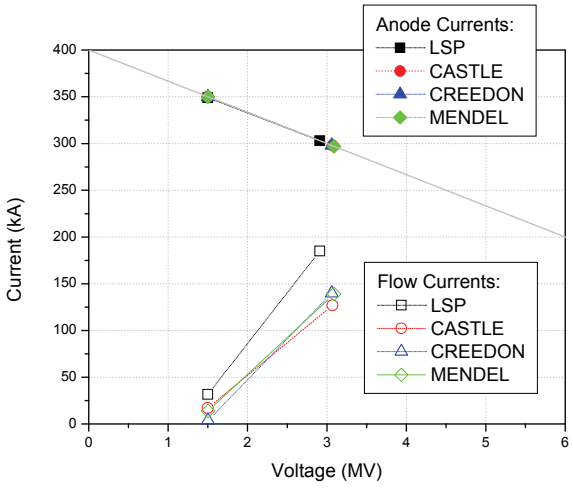

Figure 8. Comparison of currents versus voltage for the second benchmark, a good MITL transistion.

The third benchmark was much like the second, but with a 52.1-Ω MITL instead connected downstream of the 30-Ω MITL. This represents a bad transition and it was expected that flow current would be lost at this transition with higher impedance loads. The analytic solution assumes that cathode currents would be continuous across the bad transition, meaning that any change in anode current equals the loss in flow. However, PIC simulations show that this is not the case. The benchmark results, shown in Fig. 9, for the self-limited and two loaded cases, indicate that the LSP anode currents are higher than predicted by Mendel and CASTLE with higher impedance loads. The results agree only for the lowest impedance load case.

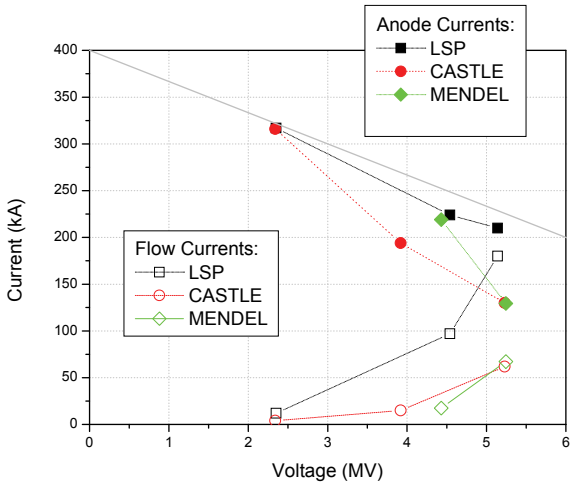

Figure 9. Comparison of anode and flow currents versus voltage for the third benchmark, a bad MITL transistion.

The disagreement between LSP and the circuit model and analytic theory stems from the assumptions that the solution would stay on the super-insulated branch, shown if Fig. 4, and that cathode currents would be continuous across the transition. Instead, the LSP results indicate that the downstream line of a bad transition is on the saturated branch with high impedance loads. It appears that the line loses only the minimum flow possible, resulting in anode currents that are nearly continuous across the transition rather than continuous cathode currents. So, until corrected, a further limitation of the MITL circuit model is that it does not work well for bad transitions.

The last benchmark, described here, compares the temporal behavior of PIC and CASTLE simulations of the existing Mercury IVA from the six feeds to a self-limited load. The feed voltage waves are all 20-ns ramps to 1.16 MV. The existing Mercury center conductor gives only good MITL transitions in the IVA so the problem with bad transitions is not an issue. Comparisons of voltages and currents at several positions in the simulations show very good agreement. Voltages and anode currents at the load are compared in Fig. 11. There is a slight difference in steady state values that is consistent with the findings of the first benchmark.

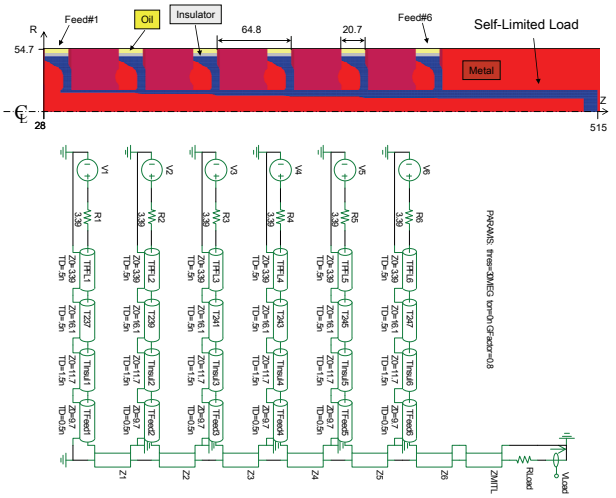

Figure 10. Setup from the PIC simulation of the Mercury IVA (above) and the equivalent CASTLE circuit schematic (below).

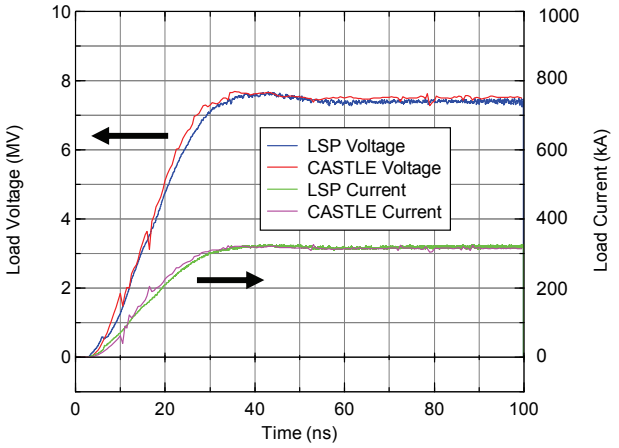

Figure 11. Comparing simulation results between LSP and CASTLE of Mercury load voltage and current.

Additional simulations were performed with a load impedance that was less than the self-limited impedance. In this case, the load voltage is reduced and a "re-trapping" [10] wave propagates upstream from the load to the generator. Although the circuit model gives the proper amplitudes for the retrapping waves, there is a discrepancy in the wave velocities between LSP and the circuit model. Retrapping wave velocities can be significantly slower than light, but in the circuit model these waves travel at the speed of light. So, a further limitation of the circuit model is that retrapping wave velocities are not accurate.

V. SIMULATION RESULTS FOR THE 8-MV MERCURY CENTER CONDUCTOR

Many PIC and CASTLE simulations were performed to explore all possibilities of modifying the Mercury center conductor for 8-MV output with minimal cost. A summary of simulation results for key sets of segment vacuum impedances are shown in Table 1 with the existing center conductor segments color coded.

Table 1. Key center conductor simulation configurations.

Simulation	$Z_0$1	$Z_0$2	$Z_0$3	$Z_0$4	$Z_0$5	$Z_0$6
Existing 7 MV	8.3	14.1	18.9	22.9	26.7	30.0
Ideal 8 MV	8.5	14.9	21.0	27.0	32.9	38.7
Keep 1,2,4,5,6	8.3	14.1	22.9	26.7	30.0	38.7
Keep 3,4,5,6	18.9	22.9	26.7	30.0	35.1	39.9
Keep 1,2	8.3	14.1	19.8	25.4	30.9	36.4
Keep 1	8.3	14.5	20.4	26.2	31.8	37.5
Keep 1,2,4,5	8.3	14.1	22.9	26.7	32.9	38.7

Simulations of the "ideal 8-MV" center conductor gave a 8.2-MV output voltage, 272-kA anode current, and 135-kA flow current. The configuration "Keep 1,2,4,5,6" in Table 1 is the most cost effective with only one new segment. It was discounted at first because circuit simulation showed bad transitions, but LSP shows there is no current loss. However, the output voltage drops to 8.0 MV and the flow current increases to 205 kA. This option will probably not be pursued because excess flow current is usually avoided in current experiments.

The "keep 3,4,5,6" option has all good transitions in the circuit code. However, a closer look reveals that the cell voltages of first three cells exceed the 1.3 MV limit, approaching 1.6 MV. The "keep 1,2" option has all good transitions, but only reaches 7.8 MV at the output. The "keep 1" option is the most expensive considered here as it uses only one original segment. It has all good transitions, but only reaches 7.9 MV at the output.

The "keep 1,2,4,5" center conductor is the most promising option. The circuit model shows slightly bad transitions, but LSP shows no current loss and the same 8.2 MV output voltage obtained with the "ideal 8-MV" center conductor. The flow current is only increased slightly to 147 kA.

VI. SUMMARY

This paper investigates simple, low cost options for modification of the Mercury center conductor to increase the nominal output voltage from 7 to 8 MV. As some of these options create a non-ideal voltage adder, simulations were required to check that cell voltage limits were not exceeded and that flow current is not lost in the adder.

A new MITL circuit model element was described. While benchmarking the MITL circuit model with LSP it was found that bad transitions do not behave as expected. The theory behind the model assumes that flow always lost at bad transitions and cathode currents are continuous. However, LSP shows that flow is often not lost and instead anode currents are nearly continuous. This is due to the downstream MITL being in the saturated branch of Mendel theory. To correctly handle bad transitions, the model will have to be modified to include the saturated branch solutions. Even with the many limitations, circuit modeling of the Mercury IVA with the new MITL circuit element allowed for more rapid simulation of various possibilities.

A review of simulation results for several possible approaches for modification of the Mercury center conductor showed that a low cost option is available. This option keeps existing center conductor segments 1, 2, 4, and 5 and adds just two new segments. Simulations have shown that this center conductor behaves nearly the same as an ideal center conductor for 8-MV output.

VII. REFERENCES

[1] R.J. Allen, et al., "Initialization and operation of Mercury, a 6-MV MIVA," 15th International Pulsed Power Conference, June 13-17, (2005).

[2] LSP is a software product of ATK Mission Research, Albuquerque, NM 87110.

[3] Ian D. Smith, "Induction voltage adders and the induction accelerator family," Phys. Rev. ST Accel. Beams, vol. 7, 064801, (2004).

[4] Private communication with Vern Bailey of L3 Pulse Sciences.

[5] John M. Creedon, "Magnetic cutoff in high-current diodes," J. Appl. Phys., vol. 48, pp. 1070-1077, (1977).

[6] P.F. Ottinger, et al., "Modeling magnetically insulated power flow in Mercury," 14th International Pulsed Power Conference, June 15-18, (2003).

[7] P.F. Ottinger and J.W. Schumer, "Rescaling of equilibrium magnetically insulated flow theory based on particle-in-cell simulations," Phys. Plasmas, vol. 13, 063101, (2006).

[8] P.F. Ottinger, et al., "Self-magnetic field effects on electron emission in planar diodes as the critical current is approached," 13th International Pulsed Power Conference, June 17-22, (2001).

[9] I. Langmuir and K. Blodgett, ''Currents limited by space charge between coaxial cylinders," Phys . Rev., vol. 22, pp. 347-356, (1923).

[10] V.L. Bailey, et al., "Re-trapping of vacuum electron current in magnetically insulated transmission lines," 15th International Conference on High-Power Particle Beams, July 18-23, (2004).